Macromolecular Bioscience
www.mbs-journal.de

Multi-Stimuli-Responsive Polymeric Prodrug for Enhanced Cancer Treatment

*Yue Wang, Na Shen, Kazuo Sakurai, and Zhaohui Tang**

Accomplishing efficient delivery of a nanomedicine to the tumor site will encounter two contradictions as follows: 1) a contradiction between prolonged circulation time and endocytosis by cancer cells; 2) a dilemma between the stability of nanomedicine during blood circulation and intracellular drug release. While developing a nanomedicine which can solve the above two contradictions simultaneously is still a challenge, here, a multi-stimuli-responsive polymeric prodrug (PLys-*co*-(PLys-DA)-*co*-(PLys-SS-PTX))-*b*-PLGLAG-mPEG (P-PEP-SS-PTX-DA) is synthesized which is multi-sensitive to overexpressed matrix metalloproteinase-2 (MMP-2), low pH, and high concentration of glutathione in tumors. The P-PEP-SS-PTX-DA can be dePEGylated and reversed from negative at normal physiological pH to positive charge at tumor extracellular microenvironment; in this way, it can solve the contradiction between prolonged circulation time and endocytosis by cancer cells. Owing to the high reductive conditions in cancer cells, P-PEP-SS-PTX-DA is ruptured to release paclitaxel (PTX) intracellular efficiently; therefore, it can resolve the dilemma between the stability of nanomedicine during blood circulation and intracellular drug release. These indicate that the multi-stimuli-responsive polymeric prodrug has potential application prospects in drug delivery and cancer therapy.

1. Introduction

Over the past few decades, nanomedicines have attracted much attention to cancer therapy.[1–7] Nanomedicine delivering active drugs to target site in a solid tumor must go through five steps: circulation in the blood, accumulation in the tumor, penetration deep into the tumor tissue, internalization by cancer cells, and intracellular drug release.[8] However, there are some obstacles in these cascaded steps,[8,9] and how to deliver sufficient drug to and inside the tumor tissue effectively is still a main challenge for cancer therapy.

There are some intractable problems still remaining in resolving the obstacles. First, there is a contradiction between prolonged circulation time and endocytosis by cancer cells. When the nanomedicines circulate in the blood, plenty of protein in the blood can bind to the surface of nanomedicines; after that they will be recognized as variants and then cleared by the reticuloendothelial system. As is well known, PEGylation can prolong circulation time, and the cancer cell endocytosis is required for nanomedicines to work. However, the PEG layer on the surface of the nanomedicines will impede their contact with the cancer cells, therefore reducing the efficiency of endocytosis. In addition, prolonging the nanomedicine blood circulation time needs slightly negative charge on the its surface; however, enhancing the cellular internalization needs positive charge on its surface.[9–13] The surface charge is a key factor in enhancing the interaction between drugs and cancer cells. Positive charge benefits drugs penetrating into tumor tissue and endocytosis by cancer cells. Second, there is a dilemma between the stability of nanomedicines during blood circulation and intracellular drug release. When nanomedicines circulate in blood, they should be stable to avoid drug burst release, but being too stable is unfavorable to efficient and complete drug release for cancer therapy.[14]

In the previous study, Liu and coworkers reported a copolymer PEG_{227}-GPLGVRG-PAsp$(DET)_{64}$ which was matrix metalloproteinase cleavable and could dePEGylate to improve cellular uptake.[15] Matrix metalloproteinases (MMPs), especially matrix metalloproteinase-2 (MMP-2) and MMP-9 are overexpressed at the invasive front of solid tumors relative to normal tissue; they are involved in many cancer invasion, progression, and metastasis.[16–18] Chen and coworkers designed a doxorubicin-loaded SNP nanomedicine which can undergo significant surface charge reversal from −7.4 to 8.2 mV at acidic tumor tissue, for enhanced uptake by cancer cells.[10] Therefore, dePEGylation and charge conversion can resolve the conflicts between prolonged blood circulation and efficient tumor cellular uptake.

Disulfide bond has been demonstrated to be stable under normal physiological conditions but can be rapidly cleaved in the tumor intracellular high concentration of glutathione

Y. Wang, Dr. N. Shen, Prof. Z. Tang
Key Laboratory of Polymer Ecomaterials
Changchun Institute of Applied Chemistry
Chinese Academy of Sciences
Changchun 130022, P. R. China
E-mail: ztang@ciac.ac.cn
Y. Wang
University of Chinese Academy of Sciences
Beijing 100049, P. R. China
Prof. K. Sakurai
The University of Kitakyushu
Department of Chemistry and Biochemistry
1-1, Hibikino, Wakamatsu-ku, Kitakyushu 808-0135, Fukuoka, Japan
The ORCID identification number(s) for the author(s) of this article can be found under https://doi.org/10.1002/mabi.201900329.

DOI: 10.1002/mabi.201900329

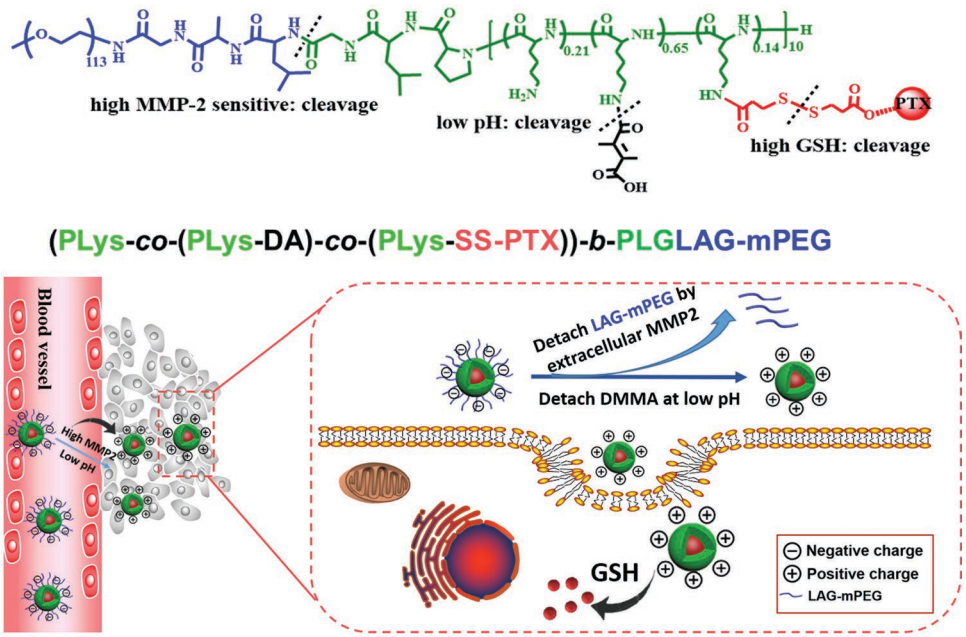

Figure 1. Illustration of multi stimuli responsive polymeric prodrug (P-PEP-SS-PTX-DA) for enhanced drug delivery.

(GSH), which is conducive to rapid release of drugs and subsequently improving the antitumor activity.[3,19–23] So, this can solve the dilemma between the stability of nanomedicine during blood circulation and intracellular drug release. Su and coworkers prepared a novel PMPC-PAEMA-P(TPE-*co*-HD)-ss-P(TPE-*co*-HD)-PAEMA-PMPC copolymer. Its structure transformation and further drug release were accelerated by high concentration of GSH in cancer cells, and obtained desirable antitumor efficacy.[24]

Developing a nanocarrier which can solve the above two contradictions simultaneously is still a challenge. In this study, we develop a multi-stimuli-responsive polymeric prodrug which can solve the above two contradictions simultaneously. A MMP-2 enzyme-sensitive polypeptide-based copolymer poly(L-lysine)-*b*-PLGLAG-methoxy poly(ethylene glycol) (PLys-*b*-PLGLAG-mPEG (P-PEP-P)) was synthesized as the polymeric scaffold. Then, HOOC-SS-PTX and DA were conjugated to P-PEP-P to form pH and redox stimuli-responsive polymeric prodrug P-PEP-SS-PTX-DA. The amide bond which is generated through amino group and a carboxylic acid group of DA is pH-sensitive and remains stable at normal physiological conditions, but is removed faster under slightly acidic conditions, so that the nanomedicines will be stable at the blood circulation and detach DA when reaching tumor slightly acidic environment, in the meantime, enzyme-sensitive polypeptide PLGLAG is cleaved by the overexpressed MMP-2 in the tumor microenvironment to dePEGylate; this can enhance cellular uptake. So, the P-PEP-SS-PTX-DA could solve the contradiction between prolonged circulation time and endocytosis by cancer cells. In addition, owing to the high reductive conditions in cancer cells, disulfide-contained nanomedicines are ruptured to release paclitaxel (PTX) intracellular efficiently (**Figure 1**). Therefore, a dilemma between the stability of nanomedicine during blood circulation and intracellular drug release is solved by the P-PEP-SS-PTX-DA. In this study, preparation and characterization of P-PEP-SS-PTX-DA as well as the in vitro cytotoxicity and cellular uptake are presented.

2. Results and Discussion

2.1. Preparation and Characterization of P-PEP-SS-PTX-DA

The preparation of P-PEP-SS-PTX-DA is shown in **Figure 2**. First, BOC-PLGLAG-OH was grafted to the amino groups of mPEG-NH_2, and then deprotection of *t*-butyloxy carbonyl groups to obtain the product H-PLGLAG-mPEG. Second, using H-PLGLAG-mPEG as a macroinitiator to synthesize PLys(Z)-*b*-PLGLAG-mPEG by ring-opening polymerization of Lys(Z)-NCA and subsequent deprotection of benzyloxycarbonyl groups to obtain P-PEP-P. Third, HOOC-SS-PTX was conjugated to P-PEP-P to receive a disulfide and peptide-containing polymeric prodrug P-PEP-SS-PTX. At last, charge-conversional unit DA was conjugated to the polymer to obtain the final product P-PEP-SS-PTX-DA.

^{1}H NMR showed that BOC-PLGLAG-OH was successfully conjugated to mPEG-NH_2 (**Figure 3**). All peaks have been assigned. The MOLDI-TOF MS spectra of BOC-PLGLAG-mPEG shows a peak at m/z = 5706.6 corresponding to the $[M+H]^+$ and at m/z = 5724.1 corresponding to the $[M+NH_4]^+$, which was consistent with the theoretical calculation value (**Figure 4**). The successful deprotection of *t*-butyloxy carbonyl groups was confirmed though the MOLDI-TOF MS, as the spectrum of H-PLGLAG-mPEG shows peak at m/z = 5555.1 corresponding to the $[M+K]^+$ and m/z = 5619.8 corresponding to the $[M+2H_2O+Na]^+$ (**Figure 5**).

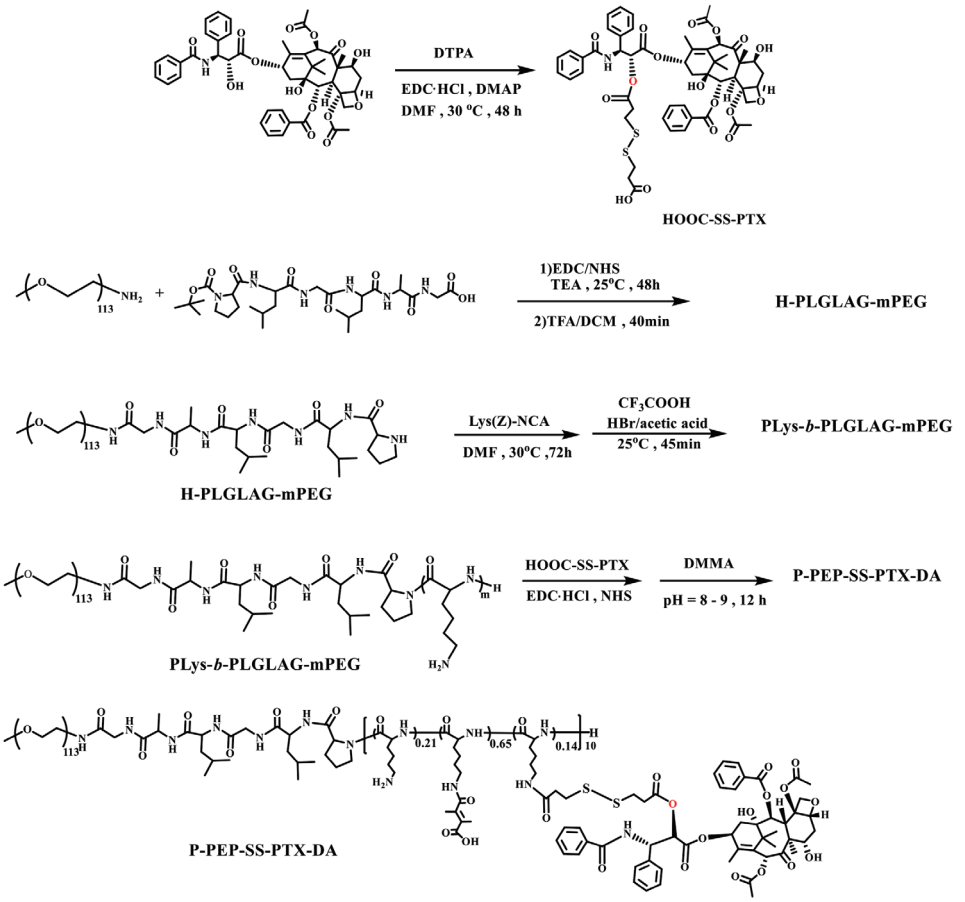

Figure 2. Synthesis of P-PEP-SS-PTX-DA.

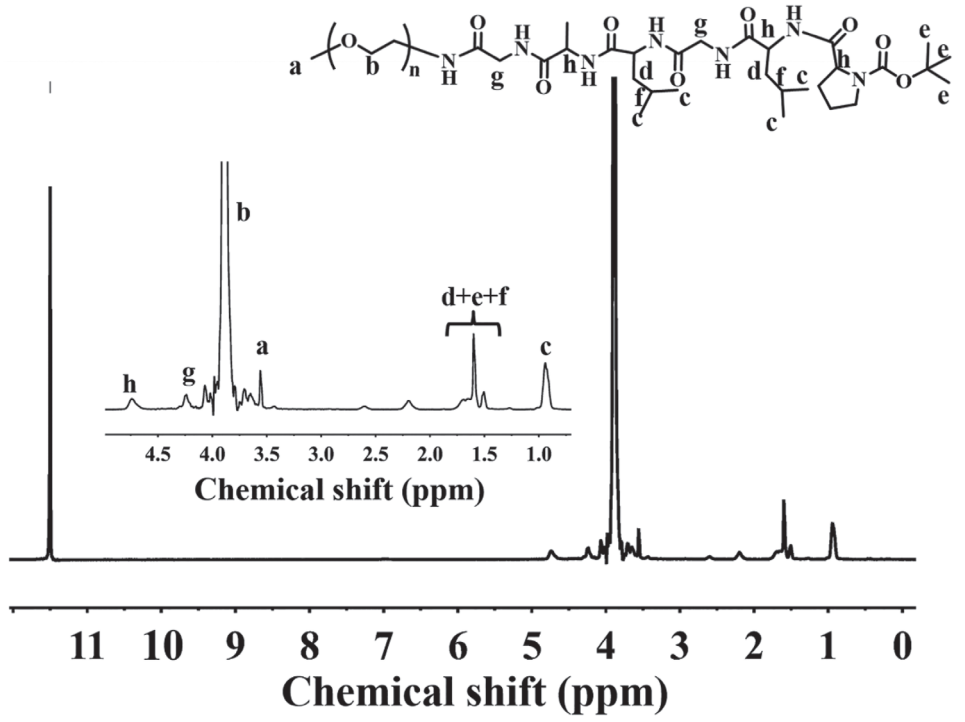

Figure 3. ^{1}H NMR spectrum of BOC-PLGLAG-mPEG in CF_3COOD.

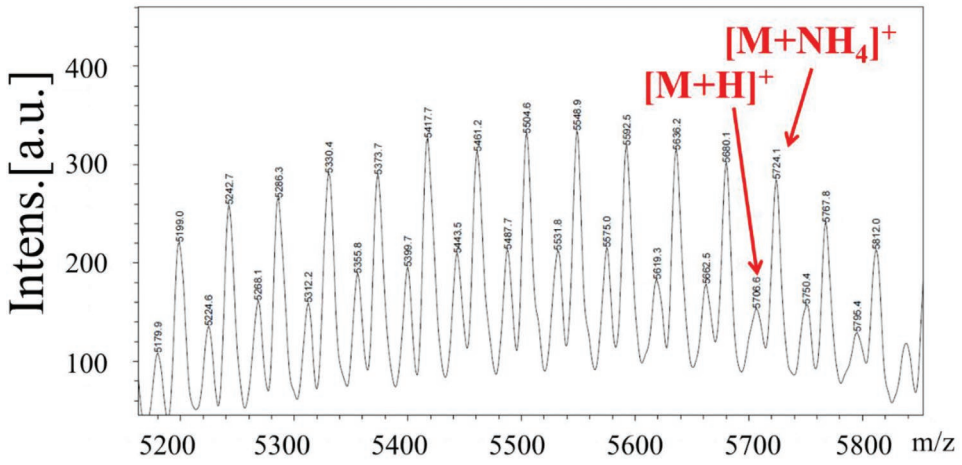

Figure 4. MOLDI-TOF MS spectrum of BOC-PLGLAG-mPEG.

The ^{1}H NMR spectra of PLys(Z)-*b*-PLGLAG-mPEG and P-PEP-P (**Figure 6**) shows that P-PEP-P was synthesized successfully. All the peaks have been well assigned. The number of Lys(Z) units in the PLys(Z)-*b*-PLGLAG-mPEG was calculated to be 10. The typical peaks of BZC groups at δ 5.08, 5.32, and 7.21 ppm disappeared, demonstrating that the deprotection process of PLys(Z)-*b*-PLGLAG-mPEG was complete.

As shown in **Figure 7**, PLGLAG was sensitive to overexpressed MMP-2; P-PEP-P can be cleaved to generate LAG-mPEG; MOLDI-TOF MS spectrum of LAG-mPEG shows peak at m/z = 5273.2 corresponding to the $[M+Na]^+$, which is entirely consistent with the theoretical calculation value. This verified that P-PEP-P was sensitive to MMP-2. This result suggested that PEG surface on the P-PEP-P micelles could be cleaved efficiently by MMP-2.

In this study, the HOOC-SS-PTX was prepared as before.[30] HOOC-SS-PTX was grafted to P-PEP-P through a condensation reaction and received P-PEP-SS-PTX which contained a disulfide bond. In **Figure 8**, the characteristic signals of phenyl proton (δ 7.2–8.0 ppm) of PTX appear in the ^{1}H NMR spectrum, demonstrating the successful conjugation of HOOC-SS-PTX to the P-PEP-P.

Finally, DA was grafted to P-PEP-SS-PTX to make the multi-stimuli-responsive nanomedicine P-PEP-SS-PTX-DA. The typical resonance of methyl(−C(C**H**$_3$)=C(C**H**$_3$)−) of DA (δ 1.64–1.87 ppm) appears in the ^{1}H NMR spectrum (**Figure 9**), indicating the successful conjugation of DA. 65% of the amine groups on PLys were replaced by DA. The DLC of PTX was calculated to be 13.3 wt% (Figure 9).

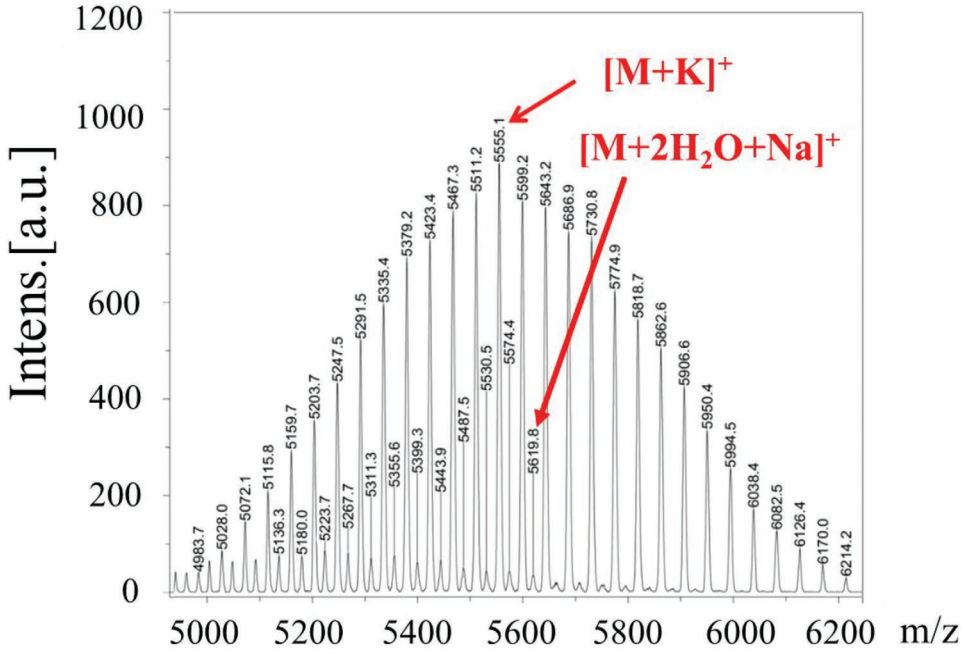

Figure 5. MOLDI-TOF MS spectrum of H-PLGLAG-mPEG.

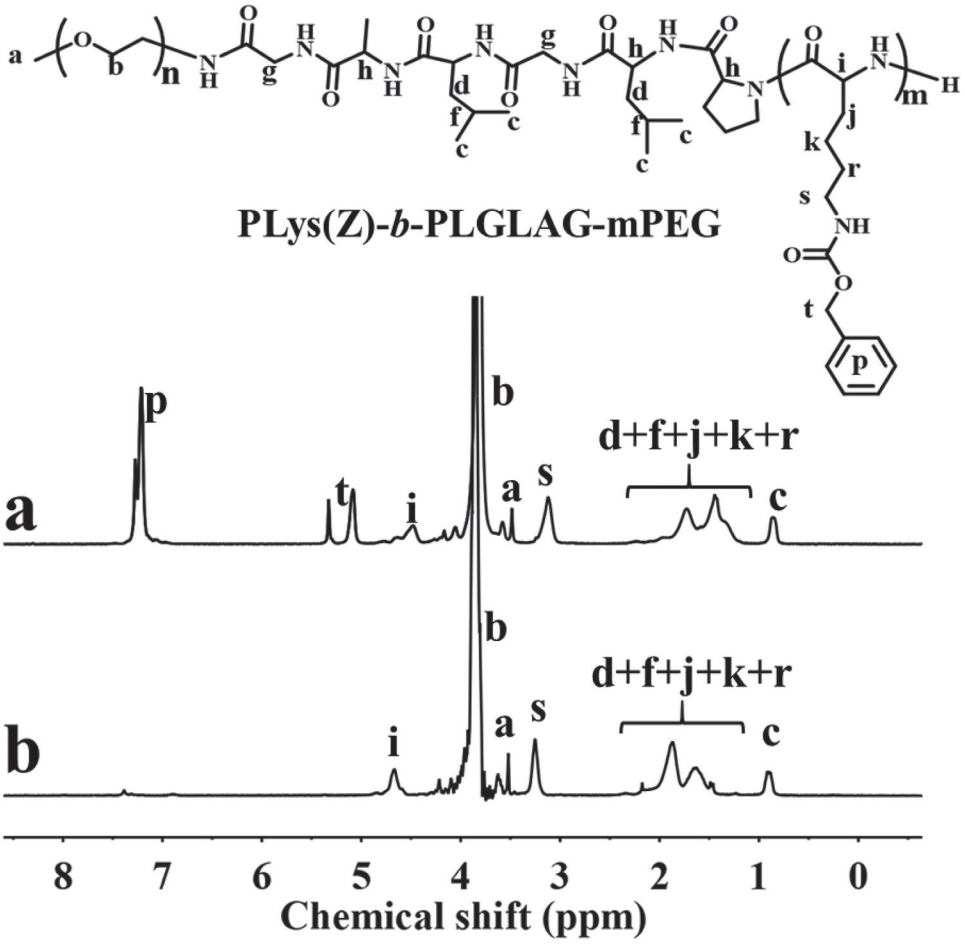

Figure 6. ^{1}H NMR spectra of PLys(Z)-*b*-PLGLAG-mPEG (a) and P-PEP-P (b) in CF_3COOD.

2.2. Dynamic Laser Scattering, pH Profile, and Zeta Potentials of P-PEP-SS-PTX-DA

In **Figure 10**a, the hydrodynamic radii (R_h) of the P-PEP-SS-PTX-DA and P-PEP-PTX-SA determined by dynamic laser scattering (DLS) were 33 ± 4 and 37 ± 4 nm, respectively. Kataoka et al. have demonstrated that the enhanced targeting of drugs to cancer cells within tumors by nanomedicines largely depends on size.[26] Especially, only nanomedicines smaller than 100 nm can penetrate poorly permeable hypovascular tumors. So, the nanomedicines we prepared in the sub-100 nm range can penetrate effectively into solid tumors.

In recent years, pH sensitive charge-conversional nanomedicines have been widely utilized for efficient drug delivery. As shown in Figure 10b, the apparent pK_b of P-PEP-SS-PTX-DA was around 7.5, so its pK_a was 6.5 as estimated from the inflexion points in the titration curves.[27] In addition, this nanomedicine exhibited a pH-buffering region of pH 7.6–6.2. Therefore, this will be conducive to the charge conversion of this nanomedicine at tumor microenvironment. The P-PEP-SS-PTX-DA nanomedicine can reverse its surface charge from negative to positive through the pH-sensitive DA groups at tumor extracellular slightly acidic condition to facilitate cell internalization. The zeta potentials of P-PEP-SS-PTX-DA at normal physiological pH (pH 7.4) and tumor tissue pH (pH 6.5) are presented in **Figure 11**a. Zeta potential of P-PEP-SS-PTX-DA increased significantly at pH 6.5, became positive in 60 min, and it was also increasing under pH 7.4 at a relatively slow rate and remained negative within 4 h. These results indicated that the P-PEP-SS-PTX-DA was negative when circulating in the blood, thus prolonging the blood circulation time. Subsequently, when it reached the slightly acidic tumor tissue set, DA would be removed with the cleavage of the amide bond and the surface of nanomedcines could be transformed to positive, thus contributing to the effective intracellular uptake of nanomedicines. In contrast, as shown in Figure 11b, the zeta potentials of control nanomedicine P-PEP-SS-PTX-SA remained negative around –15 mV within 4 h, no matter at pH 7.4 or pH 6.5. It therefore was a non-charge-conventional control which was different from P-PEP-SS-PTX-DA. This phenomenon demonstrated that P-PEP-SS-PTX-DA can overcome the contradiction between prolonged circulation time and endocytosis by cancer cells.

2.3. In vitro Release Behavior of P-PEP-SS-PTX-DA

As is well known, disulfide bonds are unstable under reductive environments.[28] To verify the effect of the reduction-sensitive

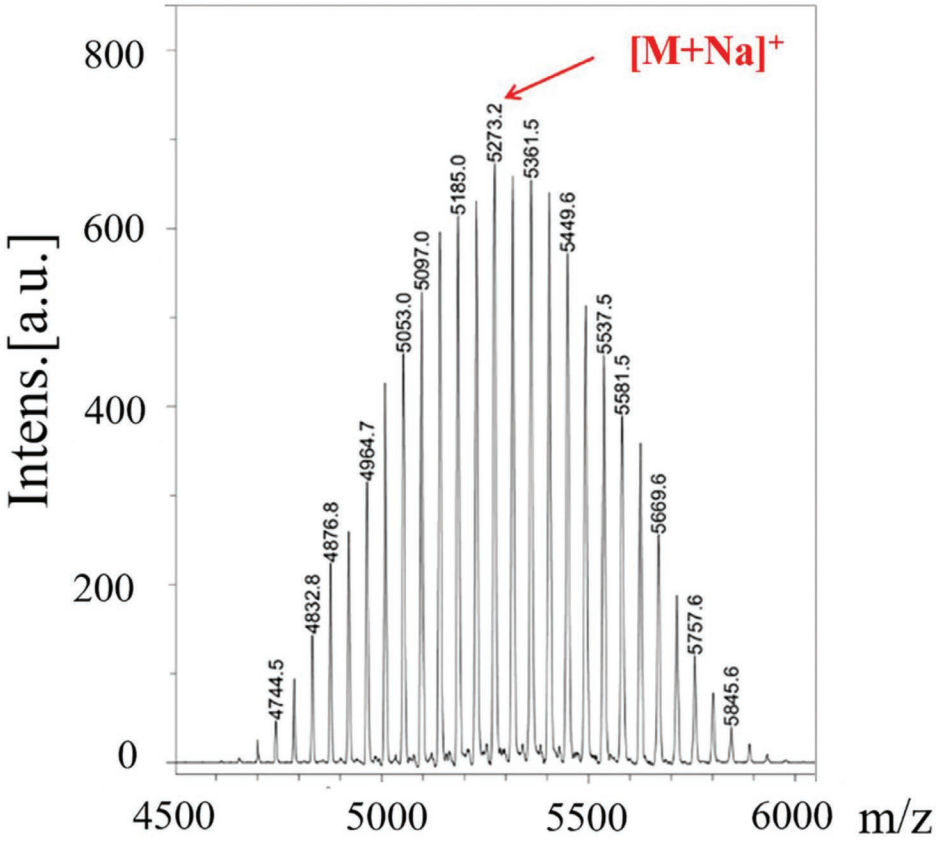

Figure 7. MOLDI-TOF MS spectrum of LAG-mPEG.

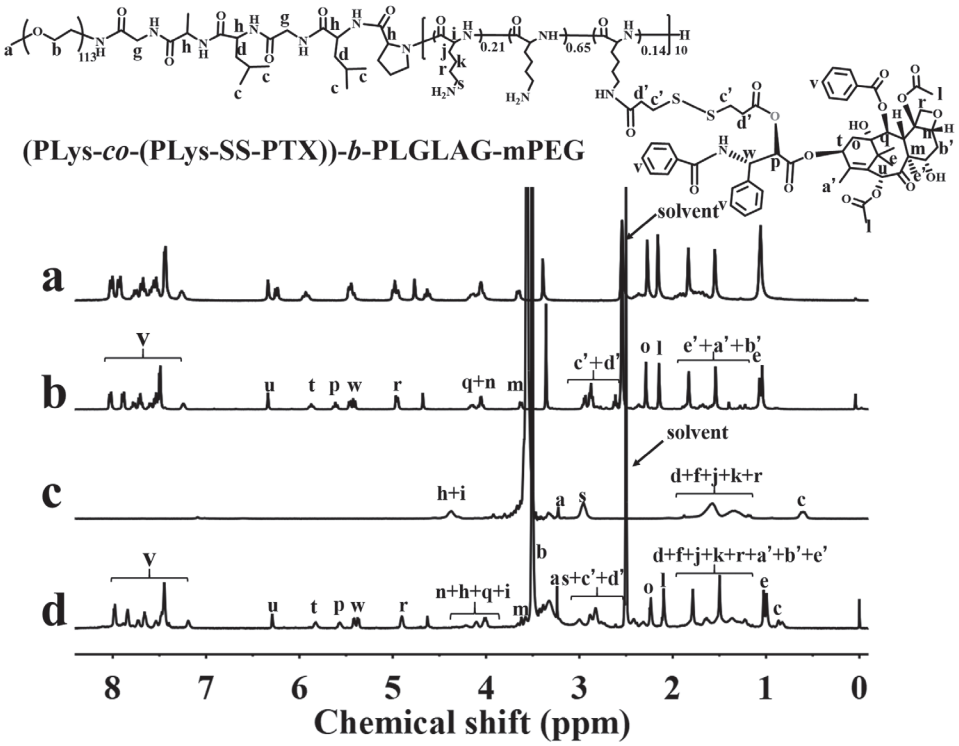

Figure 8. ^{1}H NMR spectra of PTX (a), HOOC-SS-PTX (b) in DMSO-d_6 as well as P-PEP-P (c) in CF_3COOD and the final product P-PEP-SS-PTX (d) in DMSO-d_6.

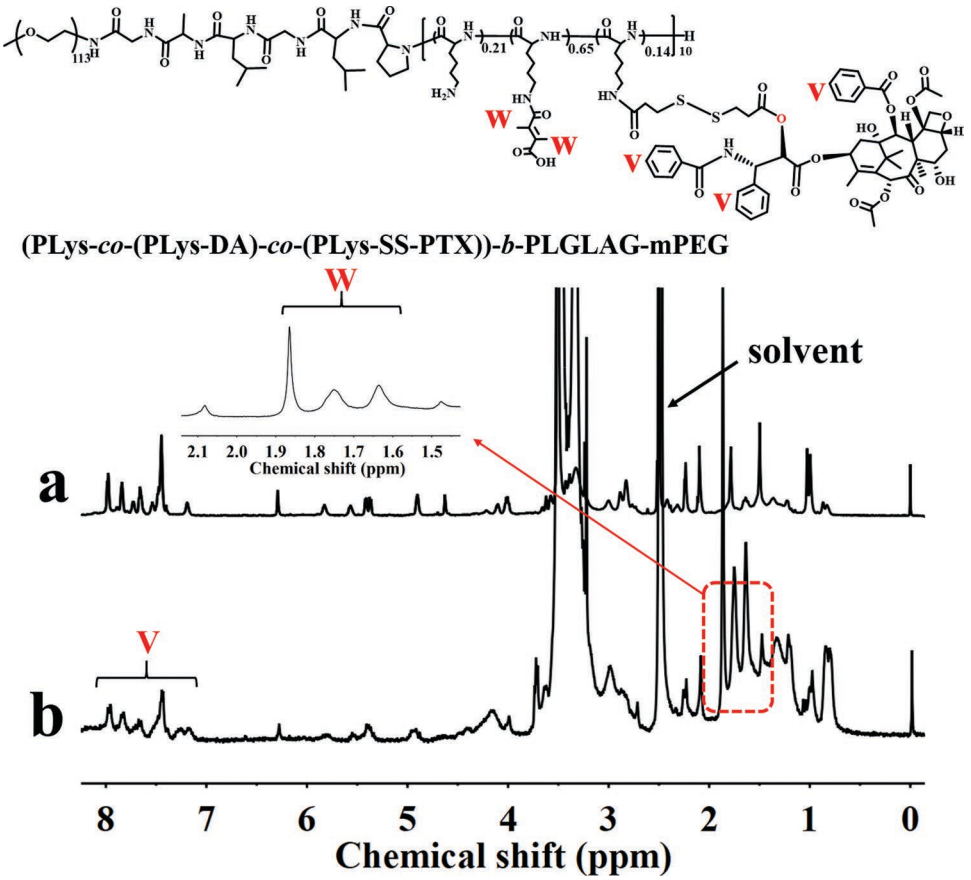

Figure 9. ^{1}H NMR spectra of P-PEP-SS-PTX (a) and P-PEP-SS-PTX-DA (b) in DMSO-d_6.

disulfide bonds on PTX release, the PTX release profiles from P-PEP-SS-PTX-DA nanomedicine were investigated at redox conditions. As shown in **Figure 12**, the PTX release from P-PEP-SS-PTX-DA nanomedicine was relatively slow at pH 7.4, only 16 wt% of conjugated PTX was released from P-PEP-SS-PTX-DA over 120 h, while almost 99 wt% of PTX was released from P-PEP-SS-PTX-DA nanomedicine in the presence of 10 mM GSH, demonstrating the redox-responsive drug release behavior of P-PEP-SS-PTX-DA nanomedicine. Therefore, it can resolve the dilemma between the stability of nanomedicine during blood circulation and intracellular drug release.

2.4. In vitro Cytotoxicity and Cellular Uptake

The in vitro cytotoxicity of P-PEP-SS-PTX-DA was studied using HT1080 cells. The cell viability was evaluated using

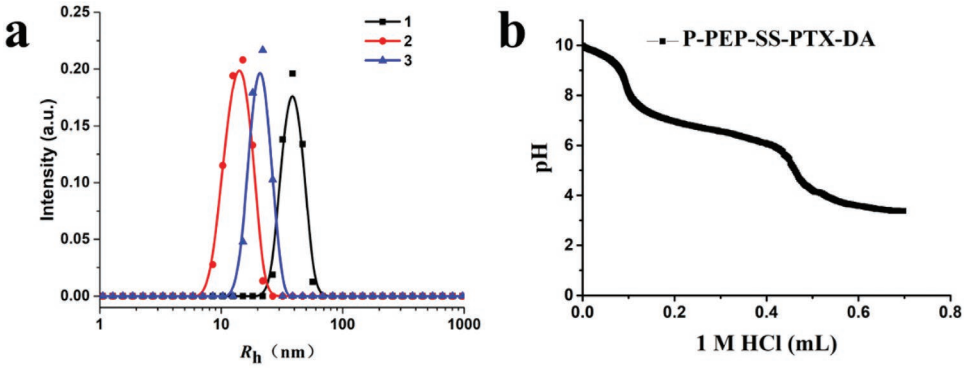

Figure 10. Size of (PLys-*co*-(PLys-SS-PTX))-*b*-PLGLAG-mPEG (1), P-PEP-SS-PTX-DA (2) and P-PEP-SS-PTX-SA (3) determined by DLS (a). The titration curve of P-PEP-SS-PTX-DA (b).

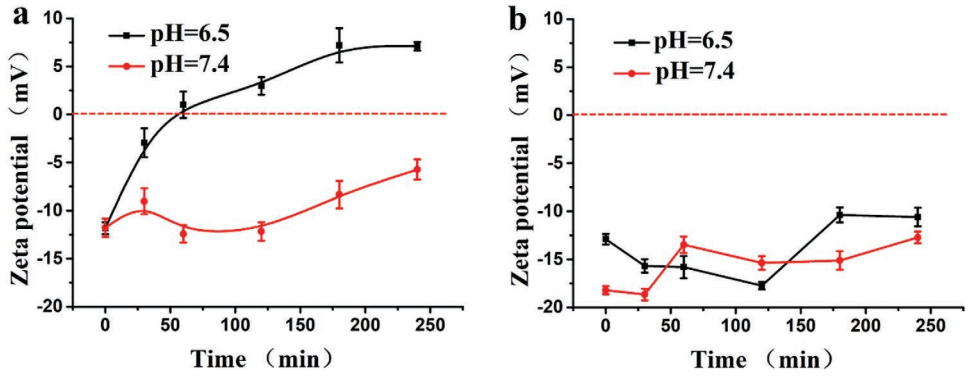

Figure 11. Zeta potentials of P-PEP-SS-PTX-DA (a) and P-PEP-SS-PTX-SA (b) at pH = 7.4 or pH = 6.5 under different incubation times. The results were represented as mean ± SD (n = 3).

MTT assay after 48 h incubation with P-PEP-SS-PTX-DA at different pH, with or without MMP-2 and GSH. As shown in **Figure 13**a, the IC_{50} values (half inhibitory concentration) of P-PEP-SS-PTX-DA under the tumor extracellular pH 6.5 was 10.5 μg PTX equivalents per milliliter, which was significantly lower than that at pH 7.4 (IC_{50} values of 43.2 μg PTX equivalents per milliliter). This indicated that P-PEP-SS-PTX-DA could change its surface charge from negative to positive at tumor extracellular pH 6.5, and thus displayed a more effective inhibition proliferation against cancer cells and solved the contradiction between prolonged circulation time and endocytosis by cancer cells. Subsequently, the cell viability of redox-sensitive P-PEP-SS-PTX-DA was investigated using MTT assay with or without GSH as demonstrated in Figure 13b. The half maximal inhibitory concentration (IC_{50}) values of P-PEP-SS-PTX-DA with 10 mM GSH was 26.3 μg PTX equivalents per milliliter, which was significantly lower than those incubated without GSH (IC_{50} values of 43.5 μg PTX equivalents per milliliter). This phenomenon indicated that the nanomedicines could effectively inhibit the cancer cell proliferation due to the redox-sensitive disulfide linkages

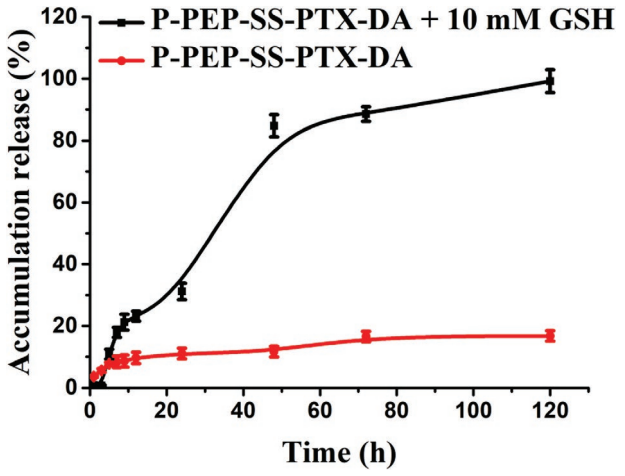

Figure 12. In vitro PTX release profiles of P-PEP-SS-PTX-DA at pH 7.4 or pH 7.4 with 10 mM GSH. The results were represented as mean ± SD (n = 3).

in the nanomedicines. This indicated that the P-PEP-SS-PTX-DA had the potential to solve the dilemma between the stability of nanomedicine during blood circulation and intracellular drug release. In addition, with the existence of MMP-2, P-PEP-SS-PTX-DA exhibited significant anti-tumor activity as revealed in Figure 13c; this was due to the MMP-2 sensitive peptide sequence PLGLAG which could be cleaved with the existence of MMP-2, thus dePEGylation improving cellular uptake.[29] IC_{50} values of P-PEP-SS-PTX-DA compared with free PTX to HT1080 cells at 48 h in different conditions are summarized in **Table 1**. The results showed that antitumor activity of P-PEP-SS-PTX-DA was comparable to that of free PTX which was attributed to the redox-responsive drug release. This could also contribute to solving the contradiction between prolonged blood circulation time and endocytosis by cancer cells.

Flow cytometry analyses further verified the phenomenon above. FITC-labeled NPs were used in the flow cytometry analysis; the fluorescence intensity was proportional to the amount of nanomedicines internalized by the cells. In **Figure 14**a, P-PEP-SS-PTX-DA and P-PEP-SS-PTX-SA exhibited a comparative mean fluorescence intensity at pH 7.4, but higher than control. This result indicated that P-PEP-SS-PTX-DA had a comparative cellular uptake compared to P-PEP-SS-PTX-SA under normal physiological environment pH 7.4. The mean fluorescence intensity of P-PEP-SS-PTX-DA with MMP-2 was given to make a quantitative comparison of the endocytosis of the nanomedicines without MMP-2. After incubation against HT1080 cells for 1 h, the nanomedicines with MMP-2 exhibited a higher fluorescence intensity than nanomedicines without MMP-2 (Figure 14b). This result showed that P-PEP-SS-PTX-DA with MMP-2 had a higher cellular uptake by the endocytosis process. P-PEP-SS-PTX-DA at different pH after incubation with HT1080 cells for 1 h is shown in Figure 14c; the mean fluorescence intensity of nanomedicines under the tumor extracellular pH 6.5 had a much higher fluorescence intensity than that under normal physiological environment pH 7.4. The results showed that nanomedicines under the tumor extracellular pH 6.5 had a higher cellular uptake compared to the nanomedicines at pH 7.4. These results demonstrated that the P-PEP-SS-PTX-DA had enhanced the cellular uptake with the existence of MMP-2 and tumoral slightly

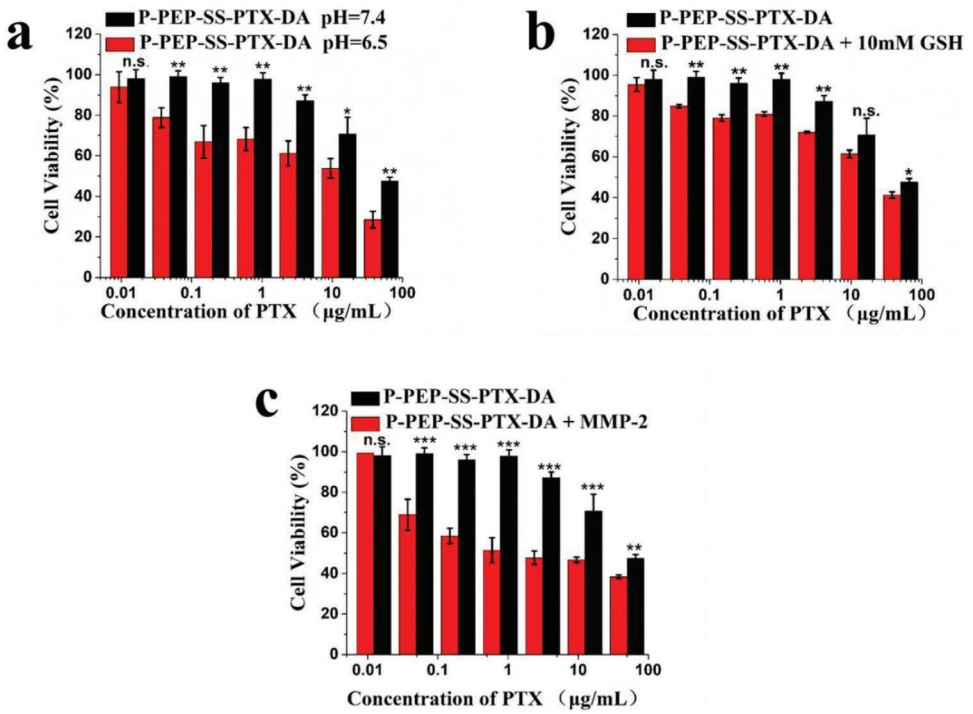

Figure 13. In vitro cytotoxicity of P-PEP-SS-PTX-DA at 48 h to HT1080 at different pH (a), P-PEP-SS-PTX-DA incubated with free or 10 mM GSH to HT1080 for 48 h (b), and P-PEP-SS-PTX-DA incubated with free or MMP-2 to HT1080 for 48 h (c). In this figure, P-PEP-SS-PTX-DA and P-PEP-SS-PTX-DA at pH 7.4 were the same. Data were represented as mean ± SD ($n = 3$). Significance levels were set using Student's *t*-test at: $^{*}p < 0.05$,$^{**}p < 0.01$, and $^{***}p < 0.001$, and n.s. was considered not significant.

acidic environment and could inhibit cancer cell proliferation effectively.

3. Conclusions

In summary, a novel multifunctional drug delivery system P-PEP-SS-PTX-DA, based on pH, GSH, and enzyme-responsive polymeric prodrug was finely designed for PTX delivery. MMP-2-triggered dePEGylation to detach LAG-mPEG and a negative charge reversed to positive on the nanomedicines' surfaces could effectively mediate cellular uptake. This had the potential to solve the contradictions between nanomedicine's prolonged blood circulation time and its endocytosis by cancer cells. Subsequently, the disulfide linkages were cleaved owing to the intracellular redox condition, which resulted in rapid drug release. This had the potential to solve the dilemma between the stability of nanomedicine during blood circulation and intracellular drug release. This indicated that the multi-stimuli-responsive drug delivery system of P-PEP-SS-PTX-DA had great potential to achieve effective cancer therapy.

4. Experimental Section

Materials: Collagenase IV (used as MMP-2) was purchased from Sigma (Shanghai, China). Dialysis bags were used with a molecular weight cutoff 3500. The other regents were performed in previous studies.[30] HOOC-SS-PTX (previously used as DTPA-PTX) was synthesized and used as previous work. The method of preparation of FITC-labeled NPs was similar as presented in previous study.[30]

Cell Culture: Fibrosarcoma HT1080 cell lines were cultured in Dulbecco's modified Eagle's medium (DMEM, Gibco). This DMEM was supplemented with 10% fetal bovine serum (FBS), penicillin (50 U mL^{-1}), and streptomycin (50 U mL^{-1}).

Synthesis of P-PEP-P: First, BOC-PLGLAG-COOH was conjugated to mPEG-NH_2 to obtain BOC-PLGLAG-mPEG, then deprotection of *t*-butyloxy carbonyl groups to obtain the product H-PLGLAG-mPEG. Briefly, BOC-PLGLAG-OH (0.200 g, 0.319 mmol), NHS (0.061 g, 0.530 mmol), and EDC·HCl (0.102 g, 0.534 mmol) were all dispersed in 15 mL dry DMF. Then, the above mixture was kept agitating for another 12 h at 25 °C.

Table 1. IC_{50} values of the PTX and P-PEP-SS-PTX-DA to HT1080 cells at 48 h in different conditions.

IC_{50} PTX [μg mL^{-1}]	pH = 7.4	pH = 6.5	pH = 7.4 + 10 mM GSH	pH = 7.4 + MMP-2
PTX	12.2	11.2	6.96	5.46
P-PEP-SS-PTX-DA	43.2	10.5	26.3	1.56

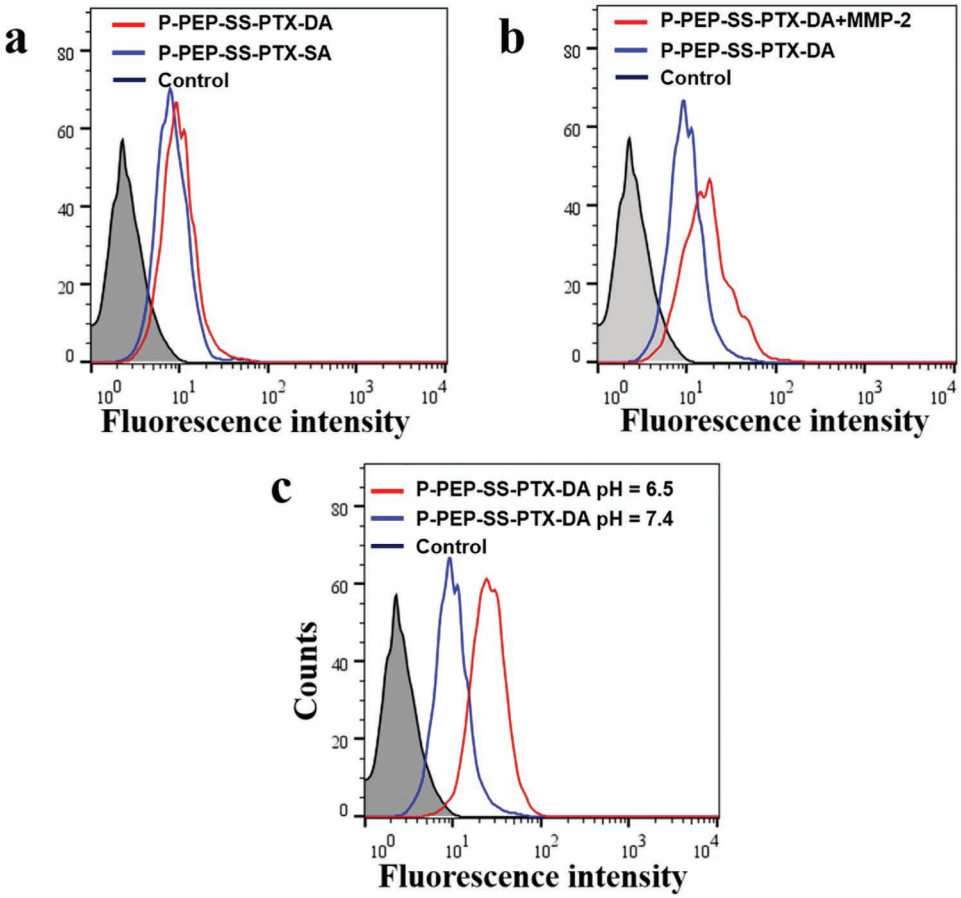

Figure 14. Flow cytometry analysis of cellular uptake. a) P-PEP-SS-PTX-DA and P-PEP-SS-PTX-SA after incubation with HT1080 cells for 1 h at pH = 7.4. b) P-PEP-SS-PTX-DA with or without MMP-2 after incubation with HT1080 cells for 1 h. c) P-PEP-SS-PTX-DA at different pH after incubation with HT1080 cells for 1 h. In this figure, P-PEP-SS-PTX-DA and P-PEP-SS-PTX-DA at pH 7.4 were the same.

Then, TEA (0.059 g, 0.531 mmol) and mPEG-NH_2 (1.330 g, 0.266 mmol) were dispersed in dry DMF, then injected into above-mentioned mixture to react for 24 h at 25 °C. The product was dialyzed, and after a lyophilization process, BOC-PLGLAG-mPEG was obtained.

H-PLGLAG-mPEG was obtained through the deprotection of *t*-butyloxy carbonyl groups on the BOC-PLGLAG-mPEG. In brief, BOC-PLGLAG-mPEG (1.07 g) was dissolved in the mixture solution of trifluoroacetic acid (18 mL) and dichloromethane (54 mL); the mixture was stirred at 25 °C; after 45 min, it was poured into cold diethyl ether. The product was then purified by dialysis against distilled water and obtained by lyophilization.

In order to obtain PLys(Z)-*b*-PLGLAG-mPEG, H-PLGLAG-mPEG was used as a macroinitiator, ring-opening polymerization of Lys(Z)-NCA was initiated, and then deprotection of benzyloxycarbonyl (BZC) groups carried out. Typically, H-PLGLAG-mPEG (0.87 g, 0.159 mmol) and Lys(Z)-NCA (1.31 g, 3.56 mmol) were dissolved in 45 mL dry DMF. The reaction solution was agitated at 30 °C under a dry nitrogen atmosphere for 3 days. At last, it was poured into cold diethyl ether to obtain PLys(Z)-*b*-PLGLAG-mPEG.

After the deprotection of BZC groups on the PLys(Z)-*b*-PLGLAG-mPEG, the P-PEP-P was obtained. Briefly, PLys(Z)-*b*-PLGLAG-mPEG (1.74 g) was mixed in TFA (18 mL) and HBr/acetic acid (33 wt%) 5.40 mL for 45 min at 25 °C. Then, it was precipitated into excessive ether and further purified by dialysis. White solid of P-PEP-P was obtained by lyophilization.

MMP-2-Triggered dePEGylation: The dePEGylation of P-PEP-P was determined by enzymatic cleavage experiment.[30] Briefly, P-PEP-P (11 mg) was dissolved in 1.0 mL of activated collagenase IV for 1 h at 37 °C. Then, the solution was extracted by dichloromethane. Finally, the product was analyzed by MOLDI-TOF MS.

Synthesis of (PLys-co-(PLys-SS-PTX))-b-PLGLAG-mPEG: A disulfide- and peptide-containing polymeric prodrug (PLys-*co*-(PLys-SS-PTX))-*b*-PLGLAG-mPEG (P-PEP-SS-PTX) was obtained through the conjugation of HOOC-SS-PTX to P-PEP-P. Briefly, HOOC-SS-PTX (0.175 g, 0.167 mmol), NHS (0.049 g, 0.426 mmol), and EDC·HCl (0.062 g, 0.325 mmol) were dispersed in 10 mL dry DMF. Then, the reaction was maintained agitating at room temperature for 12 h. Subsequently, dry DMF containing P-PEP-P (1.156 g, 0.167 mmol) and TEA (0.022 g, 0.20 mmol) were added into the above-mentioned solution. After reacting at 25 °C for 48 h, the mixture was precipitated and further purified by dialysis. P-PEP-SS-PTX was obtained after a lyophilization process.

Synthesis of P-PEP-SS-PTX-DA: Multi-stimuli-responsive polymeric prodrug P-PEP-SS-PTX-DA was prepared as follows: P-PEP-SS-PTX (0.107 g, 0.013 mmol) was dispersed in 15 mL distilled water. The mixture was adjusted to pH 8–9 by adding 0.1 M NaOH and agitated for 2 h. DA (0.051 g, 0.405 mmol) was added subsequently, during this process; the solution was kept at pH 8–9. When the pH of mixture was constant, it was stirred for another 12 h and then dialyzed. A white solid was obtained through a lyophilization process.

(PLys-*co*-(PLys-SA)-*co*-(PLys-SS-PTX))-*b*-PLGLAG-mPEG (P-PEP-SS-PTX-SA) was received through a similar way as above as a control.

In Vitro Drug Release: In vitro release of PTX from P-PEP-SS-PTX-DA was conducted in 0.01 M PBS containing 0.1% w/v Tween 80. Briefly,

P-PEP-SS-PTX-DA was dissolved in 5 mL PBS solution at pH 7.4 or pH 7.4 with 10 mM GSH, respectively, yielding a PTX concentration of 0.1 mg mL^{-1}. These samples were placed in a dialysis bag (MWCO 3500 Da) and dialyzed against 45 mL of release medium with a gently shaking rate of 100 rpm at 37 °C. 5 mL of the incubated solution was taken at predetermined times and replaced with 5 mL fresh release media. The concentration of PTX in the collected solution was tested by HPLC at 227 nm with a mobile phase of acetonitrile and water (80/20, v/v).

pH-Profile of P-PEP-SS-PTX-DA: 50 mg P-PEP-SS-PTX-DA was dissolved in 50 mL of deionized water and the pH was adjusted to 10, adding 10 µL of 1 M HCl dropwise to the above solution and recording the pH value after each drop to obtain the pH profile.

Calculation of Drug Loading Content of PTX by ^1H NMR: The drug loading content (DLC) in the P-PEP-SS-PTX-DA was calculated as follow:

PTX wt% = (Mass of PTX in P-PEP-SS-PTX-DA)/(Mass of P-PEP-SS-PTX-DA) × 100%

In vitro Cytotoxicities of P-PEP-SS-PTX-DA and P-PEP-SS-PTX-SA: The cytotoxicities of P-PEP-SS-PTX-DA and P-PEP-SS-PTX-SA against HT1080 cells were assessed by MTT assay. HT1080 cells were seeded in 96-well plates at a density of 6000 cells per well and incubated for 24 h. The medium was then replaced with 200 µL of FBS containing P-PEP-SS-PTX-DA or P-PEP-SS-PTX-SA at pH 7.4 or 6.5, with or without MMP-2, and with or without GSH. The medium was replaced with normal fresh medium after 3 h of incubation. Cell viability was measured on a Bio-Rad 680 microplate reader at a wavelength of 490 nm after another 45 h of incubation.

Cellular Uptake Measured by Flow Cytometry: HT1080 cells were seeded in 6-well plates (2×10^5 cells per well) and incubated for 24 h; then the medium was replaced with fresh DMEM containing P-PEP-SS-PTX-DA or P-PEP-SS-PTX-SA at different conditions.

Statistical Analysis: The results were expressed as mean ± standard deviation (SD) with at least three independent tests. All data were analyzed for statistical significance using Student's *t*-test. $*p < 0.05$ was considered statistically significant, $**p < 0.01$ was considered highly statistically significant, $***p < 0.001$ was considered extremely statistically significant, and n.s. was considered not significant.

Acknowledgements

This work was supported by the Ministry of Science and Technology of China (Project 2018ZX09711003-012), the National Natural Science Foundation of China (Projects 51673189), and the Jilin Province (20190103033JH).

Conflict of Interest

The authors declare no conflict of interest.

Keywords

drug delivery, matrix metallo-proteinases-2, paclitaxel, stimuli-responsive

Received: September 11, 2019
Revised: October 20, 2019
Published online: November 20, 2019

[1] J. Shi, P. W. Kantoff, R. Wooster, O. C. Farokhzad, *Nat. Rev. Cancer* **2017**, *17*, 20.
[2] S. Wang, G. Yu, Z. Wang, O. Jacobson, R. Tian, L. S. Lin, F. Zhang, J. Wang, X. Chen, *Adv. Mater.* **2018**, *30*, 1803926.
[3] Y. Huang, J. Qin, J. Wang, G. Yan, X. Wang, R. Tang, *Sci. China: Chem.* **2018**, *61*, 1447.
[4] M. Ye, Y. Han, J. Tang, Y. Piao, X. Liu, Z. Zhou, J. Gao, J. Rao, Y. Shen, *Adv. Mater.* **2017**, *29*.
[5] M. Chen, W.-G. Zhang, J.-W. Li, C.-Y. Hong, W.-J. Zhang, Y.-Z. You, *Sci. China: Chem.* **2018**, *61*, 1159.
[6] N. V. Rao, H. Ko, J. Lee, J. H. Park, *Front. Bioengin. Biotechnol.* **2018**, *6*, 110.
[7] L. Jiang, S. Zhou, X. Zhang, W. Wu, X. Jiang, *Sci. China Mater.* **2018**, *61*, 1404.
[8] Q. Sun, X. Sun, X. Ma, Z. Zhou, E. Jin, B. Zhang, Y. Shen, E. A. Van Kirk, W. J. Murdoch, J. R. Lott, T. P. Lodge, M. Radosz, Y. Zhao, *Adv. Mater.* **2014**, *26*, 7615.
[9] Q. Sun, Z. Zhou, N. Qiu, Y. Shen, *Adv. Mater.* **2017**, *29*, 1606628.
[10] J. Chen, J. Ding, Y. Wang, J. Cheng, S. Ji, X. Zhuang, X. Chen, *Adv. Mater.* **2017**, *29*, 1701170.
[11] M. Li, Y. Xu, J. Sun, M. Wang, D. Yang, X. Guo, H. Song, S. Cao, Y. Yan, *ACS Appl. Mater. Interfaces* **2018**, *10*, 10752.
[12] J. Song, C. Lin, X. Yang, Y. Xie, P. Hu, H. Li, W. Zhu, H. Hu, *J. Controlled Release* **2019**, *294*, 27.
[13] J. Zhao, S. Wu, J. Qin, D. Shi, Y. Wang, *ACS Appl. Mater. Interfaces* **2018**, *10*, 41986.
[14] H.-Y. Gong, Y.-G. Chen, X.-S. Yu, H. Xiao, J.-P. Xiao, Y. Wang, X.-T. Shuai, *Chin. J. Polym. Sci.* **2019**.
[15] J. Li, Z. Ge, S. Liu, *Chem. Commun.* **2013**, *49*, 6974.
[16] L. Zhu, F. Perche, T. Wang, V. P. Torchilin, *Biomaterials* **2014**, *35*, 4213.
[17] Q. Yao, Y. Liu, L. Kou, Y. Tu, X. Tang, L. Zhu, *Nanomed.: Nanotechnol., Biol. Med.* **2019**, *19*, 71.
[18] T. Lang, X. Dong, Z. Zheng, Y. Liu, G. Wang, Q. Yin, Y. Li, *Sci. Bull.* **2019**, *64*, 91.
[19] Y. Jiang, X. Wang, X. Liu, W. Lv, H. Zhang, M. Zhang, X. Li, H. Xin, Q. Xu, *ACS Appl. Mater. Interfaces* **2017**, *9*, 211.
[20] Y. Qu, B. Chu, X. Wei, M. Lei, D. Hu, R. Zha, L. Zhong, M. Wang, F. Wang, Z. Qian, *J. Controlled Release* **2019**, *296*, 93.
[21] Y. Gao, L. Jia, Q. Wang, H. Hu, X. Zhao, D. Chen, M. Qiao, *ACS Appl. Mater. Interfaces* **2019**, *11*, 16296.
[22] X. Ling, J. Tu, J. Wang, A. Shajii, N. Kong, C. Feng, Y. Zhang, M. Yu, T. Xie, Z. Bharwani, B. M. Aljaeid, B. Shi, W. Tao, O. C. Farokhzad, *ACS Nano* **2019**, *13*, 357.
[23] Q. Tang, J. Wang, Y. Jiang, M. Zhang, J. Chang, Q. Xu, L. Mao, M. Wang, *Chem. Commun.* **2019**, *55*, 5163.
[24] X. Su, B. Ma, J. Hu, T. Yu, W. Zhuang, L. Yang, G. Li, Y. Wang, *Bioconjugate Chem.* **2018**, *29*, 4050.
[25] N. Q. Shi, X. R. Qi, *ACS Appl. Mater. Interfaces* **2017**, *9*, 10519.
[26] H. Cabral, Y. Matsumoto, K. Mizuno, Q. Chen, M. Murakami, M. Kimura, Y. Terada, M. R. Kano, K. Miyazono, M. Uesaka, N. Nishiyama, K. Kataoka, *Nat. Nanotechnol.* **2011**, *6*, 815.
[27] E. S. Lee, K. T. Oh, D. Kim, Y. S. Youn, Y. H. Bae, *J. Controlled Release* **2007**, *123*, 19.
[28] S. Lv, Z. Tang, D. Zhang, W. Song, M. Li, J. Lin, H. Liu, X. Chen, *J. Controlled Release* **2014**, *194*, 220.
[29] L. Zhu, P. Kate, V. P. Torchilin, *ACS Nano* **2012**, *6*, 3491.
[30] Y. Wang, S. Lv, M. Deng, Z. Tang, X. Chen, *Polym. Chem.* **2016**, *7*, 2253.